

# Constraints on the winds of hot subdwarf stars from X-ray observations of two sdB binaries with compact companions: CD $-30^\circ$ 11223 and PG 1232–136

S. Mereghetti,<sup>1\*</sup> N. La Palombara,<sup>1</sup> P. Esposito,<sup>1</sup> F. Gastaldello,<sup>1,2</sup> A. Tiengo,<sup>1,3,4</sup> U. Heber,<sup>5</sup> S. Geier<sup>5,6</sup>, J. Wilms<sup>5</sup>

<sup>1</sup>INAF – Istituto di Astrofisica Spaziale e Fisica Cosmica - Milano, via E. Bassini 15, I-20133 Milano, Italy

<sup>2</sup>Department of Physics and Astronomy, University of California at Irvine, 4129, Frederick Reines Hall, Irvine, CA 926 97-4575

<sup>3</sup>IUSS – Istituto Universitario di Studi Superiori, piazza della Vittoria 15, I-27100 Pavia, Italy

<sup>4</sup>INFN – Istituto Nazionale di Fisica Nucleare - Pavia, via Bassi 6, I-27100 Pavia, Italy

<sup>5</sup>Dr. Karl Remeis-Observatory & ECAP, Friedrich-Alexander University Erlangen-Nuremberg, Sternwartstr. 7, D-96049 Bamberg, Germany

<sup>6</sup>European Southern Observatory, Karl-Schwarzschild-Str. 2, 85748 Garching, Germany

Accepted 2014 April 16. Received 2014 April 16; in original form 2014 March 21

## ABSTRACT

Little observational data are available on the weak stellar winds of hot subdwarf stars of B spectral type (sdB). Close binary systems composed of an sdB star and a compact object (white dwarf, neutron star or black hole) could be detected as accretion-powered X-ray sources. The study of their X-ray emission can probe the properties of line-driven winds of sdB stars that can not be derived directly from spectroscopy because of the low luminosity of these stars. Here we report on the first sensitive X-ray observations of two sdB binaries with compact companions. CD  $-30^\circ$  11223 is the sdB binary with the shortest known orbital period (1.2 h) and its companion is certainly a white dwarf. PG 1232–136 is an sdB binary considered the best candidate to host a black hole companion. We observed these stars with *XMM-Newton* in August 2013 for 50 ks and in July 2009 for 36 ks, respectively. None of them was detected and we derived luminosity upper limits of  $\sim 1.5 \times 10^{29}$  erg s $^{-1}$  for CD  $-30^\circ$  11223 and  $\sim 5 \times 10^{29}$  erg s $^{-1}$  for PG 1232–136. The corresponding mass loss rate for PG 1232–136 is poorly constrained, owing to the unknown efficiency for black hole accretion. On the other hand, in the case of CD  $-30^\circ$  11223 we could derive, under reasonable assumptions, an upper limit of  $\sim 3 \times 10^{-13}$  M $_{\odot}$  yr $^{-1}$  on the wind mass loss rate from the sdB star. This is one of the few observational constraints on the weak winds expected in this class of low mass hot stars. We also report the results on the X-ray emission from a cluster of galaxies serendipitously discovered in the field of CD  $-30^\circ$  11223.

## Key words:

X-rays: binaries - stars: winds, outflows – subdwarfs: individual: CD  $-30^\circ$  11223, PG 1232–136 – X-rays: galaxies: clusters: individual: XMMU J141057.7-305132

## 1 INTRODUCTION

Luminous hot stars are characterized by strong winds with mass loss rates  $\dot{M}_W \sim 10^{-7}$ – $10^{-5}$  M $_{\odot}$  yr $^{-1}$  and terminal velocities reaching a few thousands km s $^{-1}$  (see, e.g., Kudritzki & Puls 2000). These winds are driven by the resonant absorption and re-emission of the star optical/UV photons by the wind atoms, which results in a net gain of radial momentum. The theory of line-driven winds predicts that the mass-loss rate scale with the luminosity approximately as  $L^{1.5}$  and depend on the wind composition, since

most of the relevant spectral lines are provided by metals. The observations of O- and B-type stars of different luminosity, from main sequence to supergiants, agree reasonably well with these general predictions (Puls et al. 2008).

Much less is known, from the observational point of view, about the winds of less luminous hot stars, which, according to the models, should have weaker winds. Evidence of mass loss has been seen in the central stars of planetary nebulae, as well as in a few extreme helium stars and O-type subdwarfs, with  $\dot{M}_W$  as low as  $\sim 10^{-10}$  M $_{\odot}$  yr $^{-1}$  (Hamann 2010). It is not clear if the theory and scaling relations derived for luminous stars can be simply extended to such weak winds.

Hot subdwarfs are evolved low-mass stars that have lost most

\* E-mail: sandro@iasf-milano.inaf.it

of their hydrogen envelopes and are now in the stage of helium core burning (see Heber 2009 for a review). They are spectroscopically classified in the mostly hydrogen-rich sdB (with effective temperature  $T \sim 25,000\text{--}40,000$  K) and the predominantly helium-rich sdO stars (with  $T \gtrsim 40,000$  K). The abundance patterns of sdBs are strongly affected by atomic diffusion processes, that is by gravitational settling and radiative levitation leading to the depletion of some elements, e.g. helium, and strong enhancement of heavy metals by factors of up to  $10^4$  (O’Toole & Heber 2006; Blanchette et al. 2008; Naslim et al. 2011). The possible presence of winds in hot subdwarfs has been invoked to explain some of the abundance anomalies observed in these stars. Early diffusion modelling (Michaud et al. 1989) predicted that the helium abundances should be a hundred times lower than the average observed ones. Since the time scale for helium diffusion ( $\approx 10^4$  yr) is much shorter than the extreme horizontal branch (EHB) life time ( $\approx 10^8$  yr), equilibrium abundances should be established rapidly. To slow down helium diffusion, a stellar wind has been suggested (Fontaine & Chayer 1997). Indeed Unglaub & Bues (2001) showed that the observed helium abundances can be explained if a stellar wind with  $10^{-14} M_{\odot} \text{ yr}^{-1} < \dot{M}_{\text{W}} < 10^{-12} M_{\odot} \text{ yr}^{-1}$  is present. Vink & Cassisi (2002) calculated mass loss rates for EHB stars based on the line-driven wind theory and give upper limits for the mass loss rates of  $\dot{M}_{\text{W}} < 10^{-11} M_{\odot} \text{ yr}^{-1}$ . For weak mass loss rates ( $\dot{M}_{\text{W}} < 10^{-12} M_{\odot} \text{ yr}^{-1}$ ), calculations by Unglaub (2008a,b) show that the wind might fractionate, that is metals decouple from hydrogen and helium, and for rates below  $\dot{M}_{\text{W}} < 10^{-16} M_{\odot} \text{ yr}^{-1}$  become purely metallic. Since the wind is driven by metal lines, the results depend on the adopted metallicity or more precisely on the abundance of those ions that contribute most to the radiation pressure. Selective winds could explain some anomalous metal abundances, but fail to explain the observed helium abundances. An alternative explanation was offered by Michaud et al. (2011), who considered turbulent mixing of the outer  $10^{-7} M_{\odot}$  to reproduce the observed abundance anomalies.

No observational evidence for a stellar wind in a sdB star has yet been found. In optical spectra, the  $\text{H}\alpha$  line profile is the most sensitive indicator for the presence of a stellar wind. Heber et al. (2003) analysed the  $\text{H}\alpha$  line profiles of a sample of sdB and sdOB stars using the hydrostatic, fully metal line blanketed LTE model atmospheres. For all sdB stars the  $\text{H}\alpha$  profiles were matched indicating no evidence for a stellar wind. Only in the case of two sdOB stars the lines were not matched and slight asymmetries in the profile may hint at the presence of a stellar wind. Those objects, however, have already evolved off the EHB and are considerably more luminous than the sdB stars under study in this paper.

In view of the conflicting results of diffusion modelling it is of utmost importance to detect signatures of stellar winds observationally. Such an opportunity arises if the sdB is orbited by a compact companion. About two thirds of the sdB stars are in close binary systems (Maxted et al. 2001), supporting the idea that non-conservative mass transfer during a common envelope phase caused the loss of the massive hydrogen envelopes necessary to form hot subdwarfs. Both evolutionary computations and radial velocity surveys indicate that sdB binaries contain compact objects, i.e. white dwarfs (WD) or, possibly but less frequently neutron stars (NS) or black holes (Han et al. 2002; Geier et al. 2011). These systems can be detected as accretion-powered X-ray sources, if some of the mass lost from the subdwarf is transferred at a sufficiently high rate onto the compact object. Their study can thus provide a way to investigate the properties of the sdB winds, as is routinely done for more luminous O and B stars.

Up to now, the only hot subdwarfs detected in the X-ray range are two sdO stars: HD 49798 and BD +37° 442. HD 49798 is an extensively studied single-lined spectroscopic binary in a 1.5 days orbit with a 13.2 s X-ray pulsar, most likely a massive WD (Mereghetti et al. 2009). BD +37° 442 has similar optical properties, but it was believed to be a single star until the recent discovery of X-ray emission with a periodic modulation at 19.2 s (La Palombara et al. 2012), suggesting also in this case the presence of a compact companion. Compared to the majority of hot subdwarfs, HD 49798 and BD +37° 442 have relatively strong winds with  $\dot{M}_{\text{W}} \sim 3 \times 10^{-9} M_{\odot} \text{ yr}^{-1}$  (Hamann 2010). Their X-ray luminosity is consistent with the accretion rate expected from their wind properties.

A search for X-ray emission from a sample of candidate sdB+WD/NS binaries was carried out with the *Swift* satellite, but none of the targets was detected. The derived upper limits on their X-ray luminosity, of the order of  $L_{\text{X}} \sim 10^{30}\text{--}10^{31}$  erg  $\text{s}^{-1}$  (Mereghetti et al. 2011), indicate sdB mass loss rates  $\dot{M}_{\text{W}} < 10^{-13}\text{--}10^{-12} M_{\odot} \text{ yr}^{-1}$ , in the hypothesis of NS companions. On the other hand, if the compact objects in these sdB binaries are WD, the implied limits on  $\dot{M}_{\text{W}}$  are about three orders of magnitude higher and not particularly constraining.

Here we report on sensitive X-ray observations of two particularly interesting sdB binaries carried out with the *XMM-Newton* satellite. Our targets are CD -30° 11223, which is the tightest known sdB+WD binary, and PG 1232-136, which is the best candidate sdB binary with a black hole companion. We also report the results on the X-ray emission from a cluster of galaxies serendipitously discovered in the field of CD -30° 11223.

## 2 THE TARGETS

### 2.1 CD -30° 11223

The  $V=12.3$  magnitude star CD -30° 11223, spectroscopically classified as an sdB (Vennes et al. 2011), has been included among the targets of the MUCHFUSS project, which aims at finding hot subdwarf binaries with massive companions through optical spectroscopy and photometry (Geier et al. 2011). Its orbital period of 1.2 hours, by far the shortest of any sdB binary, was independently discovered by two groups (Vennes et al. 2012; Geier et al. 2013). The optical light curve shows eclipses and variations due to the ellipsoidal deformation of the sdB star caused by the tidal drag of its compact companion. Detailed modeling of these variations and extensive time-series spectroscopy led to an accurate determination of the orbital parameters and of the properties of the sdB star. Assuming that the sdB rotation is tidally locked with the orbital period, as expected for such a tight system, gives  $M_{\text{sdB}} = 0.47 \pm 0.03 M_{\odot}$  and  $M_{\text{WD}} = 0.74 \pm 0.02 M_{\odot}$  for the sdB and the WD mass, respectively. Relaxing the corotation constraint leads to slightly different values of  $M_{\text{sdB}} = 0.54 \pm 0.02 M_{\odot}$  and  $M_{\text{WD}} = 0.79 \pm 0.02 M_{\odot}$  (see Table 1 for the other parameters corresponding to these two solutions).

The very short orbital period and the certain presence of a WD companion make this system a promising target for X-ray observations. CD -30° 11223 is also interesting for its future evolution. Geier et al. (2013) proposed that it might be the progenitor of a type Ia supernova via the so-called sub-Chandrasekhar double-detonation scenario, according to which carbon burning in the core can be triggered by the ignition of helium on the surface of an accreting WD (Fink et al. 2010).

**Table 1.** Parameters of the target sdB binaries.

Parameter	Units	CD $-30^\circ$ 11223		References	PG 1232–136	References
		Solution 1	Solution 2			
Orbital period	[d]	0.048979072 $\pm$ 0.000000002		1	0.3630 $\pm$ 0.0003	2
Effective temperature	[K]	29200 $\pm$ 400		1	26900 $\pm$ 500	3
Surface gravity (log g)	[cm s $^{-2}$ ]	5.66 $\pm$ 0.05		1	5.71 $\pm$ 0.05	3
Helium abundance (log y)		–1.50 $\pm$ 0.07		1	–1.47	4
sdB mass	[ $M_\odot$ ]	0.47 $\pm$ 0.03	0.54 $\pm$ 0.02	1	0.45 <sup>a</sup>	
sdB radius	[ $R_\odot$ ]	0.169 $\pm$ 0.005	0.179 $\pm$ 0.003	1	0.16 $\pm$ 0.01	3
Companion mass	[ $M_\odot$ ]	0.74 $\pm$ 0.02	0.79 $\pm$ 0.01	1	>6	3
Companion radius	[ $R_\odot$ ]	0.0100 $\pm$ 0.0004	0.0106 $\pm$ 0.0002	1	–	
Orbital inclination	[deg]	83.8 $\pm$ 0.6	82.9 $\pm$ 0.4	1	<14	3
Orbital separation	[ $R_\odot$ ]	0.599 $\pm$ 0.009	0.619 $\pm$ 0.005	1	>4	3
Roche-lobe radius	[ $R_\odot$ ]	0.204	0.214		0.75	
Distance	[pc]	364 $\pm$ 31		1	570	5
X-ray luminosity	[erg s $^{-1}$ ]	< $1.5 \times 10^{29}$		6	< $5 \times 10^{29}$	6

References: 1) Geier et al. (2013), 2) Edelmann et al. (2005), 3) Geier et al. (2010), 4) Saffer et al. (1994), 5) Altmann et al. (2004), 6) this work  
<sup>a)</sup> Assumed value.

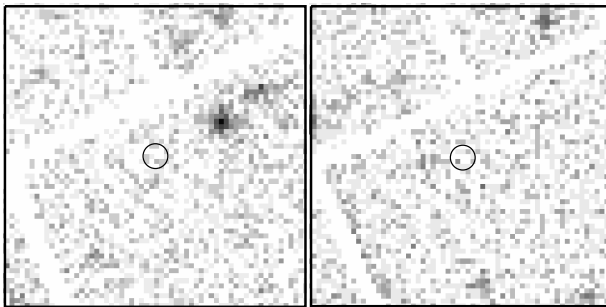


**Figure 1.** Images of the regions of CD  $-30^\circ$  11223 (left panel) and PG 1232–136 (right panel) in the 0.2–2 keV energy range obtained with the EPIC pn camera. Both images have a size of  $4 \times 4$  arcmin $^2$ , north to the top, east to the left. The positions of the two sdB binaries are indicated by the circles with radius  $10''$ .

## 2.2 PG 1232–136

PG 1232–136 is a single-lined spectroscopic binary with orbital period of 0.36 days and mass function of  $0.0819 M_\odot$  (Edelmann et al. 2005). The upper limit of  $5 \text{ km s}^{-1}$  on its projected rotational velocity, implies, with the reasonable assumption of tidally locked orbital synchronisation, a system inclination  $i < 14^\circ$ , hence a minimum companion mass of  $6 M_\odot$  (Geier et al. 2010). It is therefore very likely that the companion star of PG 1232–136 is a black hole, since any non-degenerate star of such a high mass would clearly appear in the optical spectra.

A short X-ray observation of PG 1232–136 with the *Swift*/XRT instrument gave a  $3\sigma$  upper limit of  $1.8 \times 10^{-3}$  counts s $^{-1}$  on its 0.3–10 keV count rate, which corresponds to a luminosity upper limit of  $2.6 \times 10^{30}$  erg s $^{-1}$  (Mereghetti et al. 2011). Also a search for radio emission from this system gave a negative result (Coenen et al. 2011).

## 3 OBSERVATIONS AND DATA ANALYSIS

The fields of CD  $-30^\circ$  11223 and PG 1232–136 were observed with the *XMM-Newton* satellite in August 2013 and July 2009, respectively. The details of the observations are given in Table 2.

We used the data obtained with the EPIC instrument, which consists of one pn (Strüder et al. 2001) and two MOS CCD cameras (Turner et al. 2001) operating in the 0.2–12 keV energy range. In both observations the three cameras were used in full frame mode. The medium thickness optical blocking filter was used in the MOS1 observation of CD  $-30^\circ$  11223, while all the other data were taken with the thin filter. The data were processed with Version 12 of the Standard Analysis Software (SAS).

We checked the data for the presence of high background caused by soft proton flares, finding that only the observation of PG 1232–136 was affected. We removed the corresponding time intervals, resulting in the net exposure times given in Table 2. After this standard screening of the data, we accumulated pn and MOS images in different energy bands using only single and adjacent bipixel events. Many X-ray sources were visible in these images, but none at the positions of CD  $-30^\circ$  11223 and PG 1232–136 (see Fig. 1). The closest detected sources are at angular separations of  $\sim 1'$  and  $\sim 2'$  from our targets, respectively.

To perform a more quantitative analysis and to derive luminosity upper limits for our targets, we carried out a source detection procedure over the whole field of view of the two observations. We considered the data of the three cameras simultaneously, in order to maximize the signal-to-noise ratio of the serendipitous sources and to reach lower flux limits. We first performed the source detection in the 0.5–4.5 keV energy range. For each camera, we used the cleaned event files to accumulate the field image; then we generated with the SAS task EEXPMAP the corresponding exposure map, to account for spatial quantum efficiency variations, mirror vignetting, and effective field of view. For each camera we run the SAS task EBOXDETECT in *local mode* to create a preliminary source list. Sources were identified by applying the standard *minimum detection likelihood* criterium: for each source we calculated a detection likelihood  $L = -\ln P$ , where  $P$  is the probability of a spurious detection due to a Poissonian random fluctuation of the background. We considered a threshold value  $L_{\text{th}} = 7.3$ , corresponding to a  $3\sigma$  probability that the detected counts originate from a background fluctuation. Then, the task ESPLINEMAP was run to remove all the validated sources from the original image and to create a background map by fitting the so called *cheesed image* with a cubic spline. Finally, the task EBOXDETECT was applied again in *map mode* on the three images simultaneously, using as a reference the corresponding background maps. In this way, the likelihood val-

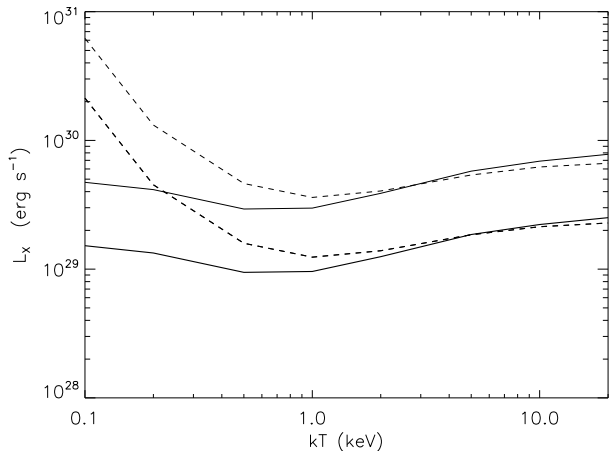


**Figure 2.** Upper limits ( $3\sigma$ ) on the 0.2–10 keV unabsorbed X-ray luminosity of CD  $-30^\circ$  11223 (lower lines) and PG 1232–136 (upper lines) for a thermal bremsstrahlung spectrum of temperature  $kT$  and  $N_{\text{H}} = 4 \times 10^{20} \text{ cm}^{-2}$ . The solid and dashed lines correspond to the count rate upper limits in the 0.2–2 keV and 0.5–4.5 keV bands, respectively.

ues from each individual instrument were converted to equivalent single-instrument detection likelihoods, and a threshold value of 7.3 was applied to accept or reject a source. In order to maximise the sensitivity for particularly soft or hard sources, we repeated the above procedure also in the energy ranges 0.2–0.5 keV, 0.2–2 keV and 2–12 keV.

No sources were detected at the position of CD  $-30^\circ$  11223 and PG 1232–136. Therefore we used the task `ESENSMAP` to create the sensitivity maps, which provide upper limits for the count rates of the undetected sources as a function of their position in the field of view. In this way we obtained  $3\sigma$  upper limits of 0.0016 and 0.0019 counts  $\text{s}^{-1}$  for the 0.5–4.5 keV count rate of CD  $-30^\circ$  11223 and PG 1232–136, respectively. Similar values were obtained for the upper limits in the other energy bands (see Table 2).

## 4 RESULTS

### 4.1 CD $-30^\circ$ 11223

No X-ray emission from CD  $-30^\circ$  11223 was detected in our observation, despite the relatively long exposure time and good sensitivity of the EPIC instrument. To convert the count rate upper limit to an X-ray luminosity it is necessary to make some assumptions on the spectral shape of the source and on the interstellar absorption. CD  $-30^\circ$  11223 is at an estimated distance of 364 pc (Geier et al. 2013) and is only slightly reddened, with  $E(B - V) = 0.04$  (Németi et al. 2012). The total column density in the direction of CD  $-30^\circ$  11223 (Galactic coordinates  $l = 322^\circ$ ,  $b = +29^\circ$ ) is  $N_{\text{H}} = 4 \times 10^{20} \text{ cm}^{-2}$  (Kalberla et al. 2005). In the following we will assume this  $N_{\text{H}}$  value for the count rate to flux conversions.

For a power-law spectrum with photon index  $\Gamma = 2$ , the count rate upper limits derived above correspond to a source flux of  $\sim 10^{-14} \text{ erg cm}^{-2} \text{ s}^{-1}$  (0.2–10 keV, corrected for the absorption). Given the source distance of 364 pc, this implies an X-ray luminosity  $L_{\text{X}} < 1.5 \times 10^{29} \text{ erg s}^{-1}$ . A thermal bremsstrahlung spectrum, as typically observed in accreting white dwarfs, leads to similar upper limits on  $L_{\text{X}}$ . These are shown in Fig. 2 as a function of the

assumed bremsstrahlung temperature  $kT$ . For temperatures below a few keV the strongest constraints are obtained by the upper limits derived in the soft spectral band image. It can be seen that for temperatures between 0.1 and 20 keV the luminosity is in the range  $(1\text{--}2) \times 10^{29} \text{ erg s}^{-1}$ . We therefore will use  $L_{\text{X}} = 10^{29} \text{ erg s}^{-1}$  as a reference normalization in the following considerations.

To derive some constraints on the mass loss rate  $\dot{M}_{\text{W}}$  from CD  $-30^\circ$  11223 based on the  $L_{\text{X}}$  upper limits, it is necessary to consider the mechanism of mass transfer and accretion possibly at work in this binary system. Even if the subdwarf radius is close to that of its Roche-lobe ( $\sim 83\%$ ), we will for simplicity consider only accretion from the stellar wind and adopt the Bondi-Hoyle formalism. In this case the accretion luminosity for a WD of mass  $M_{\text{WD}}$  and radius  $R_{\text{WD}}$  moving with velocity  $v_{\text{rel}}$  with respect to the wind is given by:

$$L_{\text{X}} = \frac{GM_{\text{WD}}}{R_{\text{WD}}} \dot{M}_{\text{W}} \left( \frac{R_{\text{a}}}{2a} \right)^2$$

where  $a$  is the orbital separation and  $R_{\text{a}} = 2GM_{\text{WD}}/v_{\text{rel}}^2$  is the accretion radius. Although this is a good approximation in high mass X-ray binaries, where  $R_{\text{a}} \ll a$ , we caution that it should be considered only as a rough estimate due to the small orbital separation of this binary. The X-ray luminosity depends on the wind velocity  $v_{\text{W}}$ , since  $v_{\text{rel}}^2 = v_{\text{o}}^2 + v_{\text{W}}^2$ , where  $v_{\text{o}} \sim 630 \text{ km s}^{-1}$  is the WD orbital velocity.

At large distances from the star, the velocity of a radiatively driven wind tends to a maximum value  $v_{\infty}$  of the order of the escape velocity. However, the wind velocity at the position of the WD is most likely smaller than  $v_{\infty}$ . For example, a typical wind velocity law  $v_{\text{W}}(R) = v_{\infty}(1 - R_{\text{sdb}}/R)^{\beta}$  with  $\beta = 1.5$  gives  $v_{\text{W}}/v_{\infty} \sim 0.6$  at  $r = a$ . Therefore we assume  $v_{\text{rel}} = 1000 \text{ km s}^{-1}$  and, for  $M_{\text{WD}} = 0.74 M_{\odot}$  and  $R_{\text{WD}} = 0.01 R_{\odot}$ , we derive the relation

$$\dot{M}_{\text{W}} = 2 \times 10^{-13} \left( \frac{L_{\text{X}}}{10^{29} \text{ erg s}^{-1}} \right) M_{\odot} \text{ yr}^{-1}$$

which can be used to convert the luminosity upper limit derived with *XMM-Newton* into a constraint on the wind mass loss rate of CD  $-30^\circ$  11223.

### 4.2 PG 1232–136

The count rate upper limits derived for PG 1232–136 from our *XMM-Newton* observation are only slightly higher than those of CD  $-30^\circ$  11223 (see Table 2). Also for this source we assumed an interstellar absorption of  $N_{\text{H}} = 4 \times 10^{20} \text{ cm}^{-2}$ , consistent with the total Galactic column density in its direction (Kalberla et al. 2005). Due to the greater distance of PG 1232–136, its flux upper limits correspond to X-ray luminosity values about three times larger than those of CD  $-30^\circ$  11223 (see Fig. 2), i.e.  $\sim 5 \times 10^{29} \text{ erg s}^{-1}$ .

To constrain  $\dot{M}_{\text{W}}$ , we assume the mass lower limit of  $6 M_{\odot}$  for the black hole companion of PG 1232–136, a wind velocity of  $1000 \text{ km s}^{-1}$  to compute the accretion radius, and an efficiency  $\eta$  for the conversion of accretion power to X-ray luminosity. In this way we find  $\dot{M}_{\text{W}} < 10^{-13} (L_{\text{X}}/5 \times 10^{29} \text{ erg s}^{-1}) (0.01/\eta) M_{\odot} \text{ yr}^{-1}$ .

**Table 2.** Log of the *XMM-Newton* observations and count rate upper limits ( $3\sigma$ ).

Target	Date (YYYY-MM-DD)	Start/end time (UT) (hh:mm)		Net exposure time (ks)			EPIC count rate (counts ks <sup>-1</sup> )			
				pn	MOS1	MOS2	0.2–0.5 keV	0.5–4.5 keV	0.2–2 keV	2–10 keV
CD –30° 11223	2013-08-17	04:19	18:45	45	51	51	<1.1	<1.6	<1.5	<1.3
PG 1232–136	2009-07-09	08:38	20:57	25	36	36	<1.4	<1.9	<1.9	<2.0

## 5 DISCUSSION AND CONCLUSIONS

Exploiting the high sensitivity of the *XMM-Newton* EPIC instrument we have carried out the first deep X-ray observations of two sdB binaries containing compact companions and obtained upper limits on their luminosity much lower than those previously available. In fact, CD –30° 11223 was never pointed before with X-ray satellites and it was not detected in the ROSAT All Sky Survey (0.1–2.4 keV). The ROSAT survey data, with an exposure of only 200 s at its position, give an upper limit of several  $10^{31}$  erg s<sup>-1</sup>. A short *Swift* observation of PG 1232–136 (Mereghetti et al. 2011) resulted in an upper limit of  $\sim 3 \times 10^{30}$  erg s<sup>-1</sup> (0.3–10 keV), for a power law with photon index  $\Gamma = 2$  (about ten times higher than that obtained here for the same spectrum).

The new upper limits on the X-ray luminosity of CD –30° 11223 and PG 1232–136, of the order of a few  $10^{29}$  erg s<sup>-1</sup> for most spectral assumptions for the count rate to flux conversion, are the most constraining ever derived for hot subdwarf binaries. Note that in the case of CD –30° 11223 the presence of a WD companion is certain, while the presence of a compact companion in PG 1232–136, as well as in most of the other sdB binaries from which X-ray emission has been searched with *Swift* (Mereghetti et al. 2011), relies on the assumption that the sdB star rotates synchronously with the orbital period (this is required to derive the system inclination which, coupled to the mass functions, leads to lower limits on the companion mass).

The lack of detectable X-ray emission in the two observed binaries can be used to derive unprecedented constraints on the wind mass loss from the hot subdwarfs in these systems. If the companion to PG 1232–136 is a black hole we have to face a large uncertainty on the conclusions that can be drawn, owing to the unknown value of the efficiency factor  $\eta$ . The low X-ray luminosity could indicate a small mass loss rate from PG 1232–136, but it could also be due to a very low efficiency in the conversion of accretion power to X-ray luminosity. This is not unexpected in the case of low rate, spherically symmetric accretion onto a black hole. It is also possible that most of the accretion luminosity is released in a different range, e.g. at much lower energies.

In the case of CD –30° 11223, however, the presence of a WD of known mass and radius allows us to make more robust considerations. The limits on  $\dot{M}_W$  we derived for this sdB are one of the few observational constraints on the weak winds expected in this class of low mass hot stars. It is interesting to make some comparison with the predictions of theoretical models. Vink & Cassisi (2002) computed the mass loss rates for horizontal branch and sdB stars expected from the theory of radiation driven winds. They derived a scaling relation linking  $\dot{M}_W$  with the star’s effective temperature, luminosity, mass and metallicity. For the parameters of CD –30° 11223 this relation yields a mass loss rate  $\dot{M}_W = 1.2 \times 10^{-12} Z^{0.97} M_\odot \text{ yr}^{-1}$ , where  $Z$  is the metallicity. Hamann (2010) derived a mass loss vs. luminosity relation for evolved hot, low mass stars, which are more than ten times as luminous as the sdB stars. Extrapolation of that relation (Fig. 10 of Hamann (2010)) yields a mass loss rate for CD –30° 11223 consistent with the pre-

diction of Vink & Cassisi (2002). Our derived upper limit on  $\dot{M}_W$ , of the order of  $3 \times 10^{-13} M_\odot \text{ yr}^{-1}$  for most spectral assumptions, seems difficult to reconcile with the prediction by Vink & Cassisi (2002) if CD –30° 11223 has a solar, or higher, metallicity. The metal abundance pattern of CD –30° 11223 (and PG 1232–136) has not yet been determined. In order to make a more meaningful comparison, it would be most important to determine the abundances of heavy elements such as iron, nickel and trans-iron elements, the lines of which dominate the radiation pressure for sdB stars. This determination requires high-resolution UV spectroscopy (see, e.g., O’Toole & Heber 2006). We finally note that our upper limit on  $\dot{M}_W$  is in the range of mass loss rates which, according to Unglaub & Bues (2001), can explain the He abundances of sdB stars.

## APPENDIX A: THE SERENDIPITOUS DETECTION OF X-RAY EMISSION FROM THE CLUSTER OF GALAXIES XMMU J141057.7-305132

An extended source in the field of CD –30° 11223 is clearly detected at  $4'$  off-axis (see Fig.A1). The most likely interpretation is that of X-ray emission from a cluster of galaxies. Based on the position of its X-ray centroid ( $\alpha_{J2000} = 14^{\text{h}}10^{\text{m}}57^{\text{s}}.7$ ,  $\delta_{J2000} = -30^\circ 51' 32''.3$ ), we denote it XMMU J141057.7-305132. There are no redshifts in *NED* possibly associated with this source, except for the galaxy 2MASX J14104995-3052321, which is at a distance of  $2'$ , therefore outside the visible extent of the diffuse X-ray emission; its redshift of  $z = 0.0619$  is too close given also the indication of the redshift obtained from the X-ray data (see below). All the errors quoted in this Appendix are at the 68% confidence limit and all distance-dependent quantities have been computed assuming  $H_0 = 70 \text{ km s}^{-1} \text{ Mpc}^{-1}$ ,  $\Omega_m = 0.3$  and  $\Omega_\Lambda = 0.7$ .

For each detector we created images in the 0.5–2 keV band with point sources masked using circular regions of  $25''$  radius. Only for three sources embedded in the diffuse emission we used an exclusion radius of  $20''$  (corresponding to 80% of the encircled energy fraction at 1.5 keV for a point source at this off-axis angle). In particular we excluded a hard source (at  $\alpha_{J2000} = 14^{\text{h}}10^{\text{m}}56^{\text{s}}$ ,  $\delta_{J2000} = -30^\circ 51' 03''$ ) clearly visible in the 2–5 keV image. The images have been exposure corrected and a radial surface brightness profile has been extracted from a circular region of  $6'$  radius centered on the cluster position. We account for the X-ray background in the surface brightness analysis by including a constant-background component. The data were grouped to have at least 20 counts per bin in order to apply the  $\chi^2$  statistics. The fitted model is convolved with the *XMM-Newton* point spread function (PSF). The joint best-fit  $\beta$ -model (Cavaliere & Fusco-Femiano 1976) has a core radius of  $r_c = 56'' \pm 7''$  and  $\beta = 0.76 \pm 0.08$  for a  $\chi^2/\text{dof} = 287/205$  (see Fig. A2). The main contribution to the  $\chi^2$  comes from the pn and its origin is instrumental (CCD gaps).

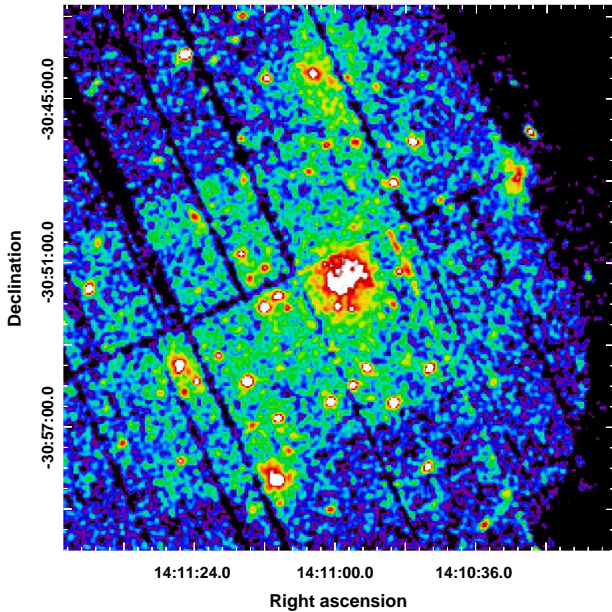


**Figure A1.** EPIC X-ray image in the 0.5–2.0 keV energy band of a  $20' \times 20'$  region around the the cluster XMMU J141057.7-305132 (see the online journal for a color version of this figure).

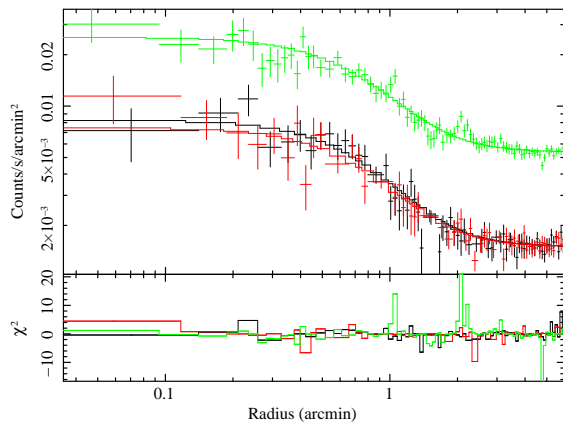


**Figure A2.** Surface brightness profile of the X-ray emission of XMMU J141057.7-305132. Top panel: data and best fit beta model. Bottom panel: contribution of each data point to the total  $\chi^2$ . Data from MOS1, MOS2 and pn are plotted in black, red and green respectively (see the online journal for a color version of this figure).

For spectral fitting, we extracted spectra for each detector from a region with  $1.5'$  radius centered on the emission centroid. Redistribution matrix files (RMFs) and ancillary response files (ARFs) were generated using the SAS tasks RMFGEN and ARFGEN in extended source mode with appropriate flux weighting. The background was estimated locally using spectra extracted from a source free region of the same extent at the same off-axis angle. This is particularly relevant since the field is in a region (Galactic coordinates  $l = 322.43^\circ$ ,  $b = +28.99^\circ$ ) of enhanced Galactic foreground (see the ROSAT R45 map of Snowden et al. 1997).

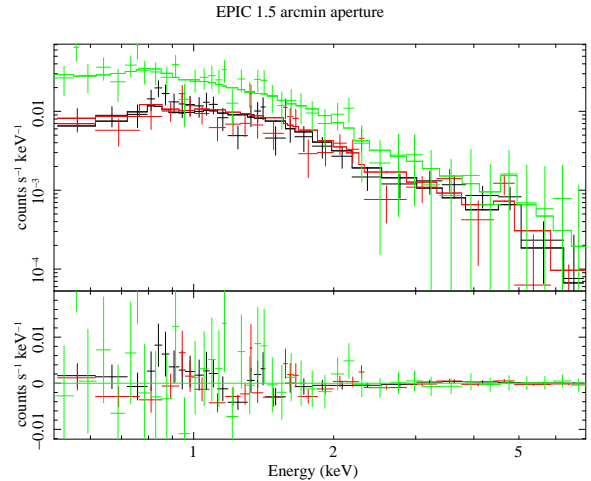


**Figure A3.** X-ray spectra of the XMMU J141057.7-305132 taken from a  $1.5'$  radius aperture centered on the centroid of the emission. The best fit model and residuals are also shown. Data from MOS1, MOS2 and pn are plotted in black, red and green respectively (see the online journal for a color version of this figure).

The spectra from the three detectors were jointly fitted with an APEC thermal plasma (Smith et al. 2001) with Galactic absorption fixed at  $N_{\text{H}} = 4 \times 10^{20} \text{ cm}^{-2}$  (Kalberla et al. 2005). The spectral fitting was performed in the 0.5–7 keV band using the C-statistic and quoted metallicities are relative to the abundances of Anders & Grevesse (1989). The spectra are shown in Fig.A3: we fixed the metallicity at  $Z = 0.3 Z_{\odot}$  and the best fit parameters are  $kT = 4.1 \pm 0.3 \text{ keV}$  and  $z = 0.38 \pm 0.01$  for a C-stat/dof = 766/716. The X-ray determinations of the redshift have been proven to be sufficiently reliable when compared with optical redshifts (e.g., Gastaldello et al. 2007; Panessa et al. 2009): in the following we will therefore assume  $z = 0.38$  as the redshift of the source, for which  $1'$  corresponds to 311 kpc. We obtained a flux of  $(8.94 \pm 0.28) \times 10^{-14} \text{ erg cm}^{-2} \text{ s}^{-1}$  in the 0.5–2 keV band in the  $1.5'$  aperture, increased by 12% due to the area lost for the point source exclusion. The source photons correspond to about 50% of the total events ( $\sim 1500$  counts in each MOS and 3400 in the pn).

Under the assumption of isothermality we can calculate the total mass profile using the best-fit  $\beta$ -model ( $r_c = 290 \pm 36 \text{ kpc}$ ), for which the gas density and total mass profiles can be expressed by simple analytical formulae (e.g. Ettori 2000). We evaluated  $r_{500}$  as the radius at which the density is 500 times the critical density and the virial radius as the radius at which the density corresponds to  $\Delta_{\text{vir}}$ , as obtained by Bryan & Norman (1998)<sup>1</sup> for the concordance cosmological model used in this paper. To evaluate the errors on the estimated quantities we used the procedure of repeating the measurements for 10000 random selections drawn from Gaussian distributions for the temperature and parameters of the surface brightness profile. For  $\Delta = 500$  we obtained,  $M_{500} = (2.67 \pm 0.59) \times 10^{14} M_{\odot}$  within  $r_{500} = 857 \pm 63 \text{ kpc}$ ; the virial mass is,  $M_{\text{vir}} = (5.90 \pm 1.18) \times 10^{14} M_{\odot}$ , within the virial radius  $r_{\text{vir}} = 1747 \pm 116 \text{ kpc}$ . For XMMU J141057.7-305132, the aperture of

<sup>1</sup>  $\Delta_{\text{vir}} = 18\pi^2 + 82x - 39x^2$  where  $x = \Omega(z) - 1$ ,  $\Omega(z) = \Omega_{\text{m}}(1+z)^3/E(z)^2$  and  $E(z) = [\Omega_{\text{m}}(1+z)^3 + \Omega_{\Lambda}]^{1/2}$ .

467 kpc used for spectroscopy encloses 76% of the flux within  $r_{500}$ . The derived bolometric luminosity within  $r_{500}$  is  $L_{500} = (1.19 \pm 0.11) \times 10^{44} \text{ erg s}^{-1}$ . Given also the limited radial range in which the luminosity and, in particular, the temperature have been obtained we can only estimate that the self-similar scaled value of  $E(z)^{-1} L_{500}$  for XMMU J141057.7-305132 is in agreement with the local  $L_X-T_X$  relations (Markevitch 1998; Arnaud & Evrard 1999; Pratt et al. 2009), with an indication of being slightly underluminous, which might be consistent with recent claims of a negative evolution of the  $L_X-T_X$  relation (Reichert et al. 2011).

#### ACKNOWLEDGMENTS

We acknowledge the financial support by the Italian Space Agency through the ASI/INAF agreement I/032/10/0 for the XMM-Newton operations. This research is based on data of XMM-Newton, an ESA science mission with instruments and contributions directly funded by ESA Member States and NASA.

#### REFERENCES

- Altmann M., Edelmann H., de Boer K. S., 2004, *A&A*, 414, 181
- Anders E., Grevesse N., 1989, *Geochim. Cosmochim. Acta*, 53, 197
- Arnaud M., Evrard A. E., 1999, *MNRAS*, 305, 631
- Blanchette J.-P., Chayer P., Wesemael F., Fontaine G., Fontaine M., Dupuis J., Kruk J. W., Green E. M., 2008, *ApJ*, 678, 1329
- Bryan G. L., Norman M. L., 1998, *ApJ*, 495, 80
- Cavaliere A., Fusco-Femiano R., 1976, *A&A*, 49, 137
- Coenen T., van Leeuwen J., Stairs I. H., 2011, *A&A*, 531, A125
- Edelmann H., Heber U., Altmann M., Karl C., Lisker T., 2005, *A&A*, 442, 1023
- Ettori S., 2000, *MNRAS*, 311, 313
- Fink M., Röpke F. K., Hillebrandt W., Seitenzahl I. R., Sim S. A., Kromer M., 2010, *A&A*, 514, A53
- Fontaine G., Chayer P., 1997, in Philip A. G. D., Liebert J., Saffer R., Hayes D. S., eds, *The Third Conference on Faint Blue Stars The Helium Abundance Puzzle in Subdwarf B Stars: a Theoretical Interpretation Through Mass Loss*. p. 169
- Gastaldello F., Buote D. A., Humphrey P. J., Zappacosta L., Seigar M. S., Barth A. J., Brighenti F., Mathews W. G., 2007, *ApJ*, 662, 923
- Geier S., et al., 2013, *A&A*, 554, A54
- Geier S., Heber U., Podsiadlowski P., Edelmann H., Napiwotzki R., Kupfer T., Müller S., 2010, *A&A*, 519, A25
- Geier S., Hirsch H., Tillich A., Maxted P. F. L., Bentley S. J., Østensen R. H., Heber U., Gänsicke B. T., Marsh T. R., Napiwotzki R., Barlow B. N., O’Toole S. J., 2011, *A&A*, 530, A28
- Hamann W.-R., 2010, *Ap&SS*, 329, 151
- Han Z., Podsiadlowski P., Maxted P. F. L., Marsh T. R., Ivanova N., 2002, *MNRAS*, 336, 449
- Heber U., 2009, *ARA&A*, 47, 211
- Heber U., Maxted P. F. L., Marsh T. R., Knigge C., Drew J. E., 2003, in Hubeny I., Mihalas D., Werner K., eds, *Stellar Atmosphere Modeling Vol. 288 of Astronomical Society of the Pacific Conference Series, Stellar Wind Signatures in sdB Stars?*. p. 251
- Kalberla P. M. W., Burton W. B., Hartmann D., Bajaja E., Morras R., Pöppel W. G. L., 2005, *A&A*, 440, 775
- Kudritzki R.-P., Puls J., 2000, *ARA&A*, 38, 613
- La Palombara N., Mereghetti S., Tiengo A., Esposito P., 2012, *ApJ*, 750, L34
- Markevitch M., 1998, *ApJ*, 504, 27
- Maxted P. F. L., Heber U., Marsh T. R., North R. C., 2001, *MNRAS*, 326, 1391
- Mereghetti S., Campana S., Esposito P., La Palombara N., Tiengo A., 2011, *A&A*, 536, A69
- Mereghetti S., Tiengo A., Esposito P., La Palombara N., Israel G. L., Stella L., 2009, *Science*, 325, 1222
- Michaud G., Bergeron P., Wesemael F., Heber U., 1989, *ApJ*, 338, 417
- Michaud G., Richer J., Richard O., 2011, *A&A*, 529, A60
- Naslim N., Jeffery C. S., Behara N. T., Hibbert A., 2011, *MNRAS*, 412, 363
- Németh P., Kawka A., Vennes S., 2012, *MNRAS*, 427, 2180
- O’Toole S. J., Heber U., 2006, *A&A*, 452, 579
- Panessa F., Carrera F. J., Bianchi S., Corral A., Gastaldello F., Barcons X., Bassani L., Matt G., Monaco L., 2009, *MNRAS*, 398, 1951
- Pratt G. W., Croston J. H., Arnaud M., Böhringer H., 2009, *A&A*, 498, 361
- Puls J., Vink J. S., Najarro F., 2008, *A&A Rev.*, 16, 209
- Reichert A., Böhringer H., Fassbender R., Mühlegger M., 2011, *A&A*, 535, A4
- Saffer R. A., Bergeron P., Koester D., Liebert J., 1994, *ApJ*, 432, 351
- Smith R. K., Brickhouse N. S., Liedahl D. A., Raymond J. C., 2001, *ApJ*, 556, L91
- Snowden S. L., Egger R., Freyberg M. J., McCammon D., Plucinsky P. P., Sanders W. T., Schmitt J. H. M. M., Truemper J., Voges W., 1997, *ApJ*, 485, 125
- Strüder L., Briel U., Dennerl K., et al. 2001, *A&A*, 365, L18
- Turner M. J. L., Abbey A., Arnaud M., et al. 2001, *A&A*, 365, L27
- Unglaub K., 2008a, *A&A*, 486, 923
- Unglaub K., 2008b, in Heber U., Jeffery C. S., Napiwotzki R., eds, *Hot Subdwarf Stars and Related Objects Vol. 392 of Astronomical Society of the Pacific Conference Series, The Mass Loss Rates of sdB Stars*. p. 95
- Unglaub K., Bues I., 2001, *A&A*, 374, 570
- Vennes S., Kawka A., Németh P., 2011, *MNRAS*, 410, 2095
- Vennes S., Kawka A., O’Toole S. J., Németh P., Burton D., 2012, *ApJ*, 759, L25
- Vink J. S., Cassisi S., 2002, *A&A*, 392, 553

This paper has been typeset from a  $\text{\TeX}/\text{\LaTeX}$  file prepared by the author.